Collision Avoidance Strategies for Unmanned Aerial Vehicles in Formation Flight

Joongbo Seo, Youdan Kim, Seungkeun Kim and Antonios Tsourdos, *Member, IEEE*

Abstract—Collision avoidance strategies for multiple UAVs (Unmanned Aerial Vehicles) based on geometry are investigated in this study. The proposed strategies allow a group of UAVs to avoid obstacles and separate if necessary through a simple algorithm with low computation by expanding the collision-cone approach to formation of UAVs. The geometric approach uses line-of-sight vectors and relative velocity vectors where dynamic constraints are included in the formation.Each UAV can determine which plane and direction are available for collision avoidance. An analysis is performed to define an envelope for collision avoidance, where angular rate limits and obstacle detection range limits are considered. Based on the collision avoidance envelope, each UAV in a formation determines whether the formation can be maintained or not while avoiding obstacles. Numerical simulations are performed to demonstrate the performance of the proposed strategies.

Index Terms—Unmanned Aerial Vehicle(UAV), collision avoidance, decision making, formation keeping, formation splitting.

I. INTRODUCTION

Use of multiple UAVs has a potential merit in military, governmental and commercial real-world tasks : intelligence, surveillance and reconnaissance, border patrol, threat detection, target tracking, search and rescue, atmospheric research due to its inherent redundancy and cooperativeness.[1-6] Note that multiple UAVs can perform various complicated missions efficiently and effectively. Multiple aircraft in close formation with precisely defined geometry also have advantage of energy saving when the vortex forces are considered. [7]. In military tactical formation flight, aircraft usually perform various manoeuver such as turning, acceleration, and deceleration, and therefore each formation members need to have enough formation distance. [8] Also, formation flight may be useful for airborne refueling and quick deployment of troops and vehicles [9]. To perform those missions, UAVs must have functions of avoiding other aircraft and obstacles. One of the major challenges in the military mission is the risk of unintentional collision between UAVs and/or manned aircraft. Therefore, collision avoidance has become increasingly important for the safe operation of UAVs, particularly for integration into the civilian airspace. Collision avoidance algorithms can be classified into three approaches: optimization methods, force-field methods, and sense-and-avoid methods.

Optimization methods attempt to find an input that minimizes a performance index to avoid obstacles. [10], [11] Most of these methods calculate the performance index for a finite time horizon, which can be easily combined with model predictive control as in [12-16]. However, receding horizon control has some inherent disadvantages coming from absence of state information over the finite time horizon. Smith *et al.* developed a general framework to pose a collision avoidance problem of remotely piloted aircrafts as an optimal control problem using a stochastic estimator, [17], [18] where they used particle filter to minimize the effects of uncertainty caused by pop-up circumstances and to enable real-time implementation. Sujit *et al.* developed a path planning algorithm for multiple UAVs with limited sensor and communication ranges. [19] They used particle swarm optimization to avoid detected static and pop-up obstacles.

Because the particle swarm optimization includes theprocess of update and iteration in a finite time step, the algorithm can improve its quality of solution with a given sufficient amount of time. George *et al.* and Manathara *et al.* proposed a decentralized optimal coalition formation algorithm for multiple targets.[20-22] In their research, decentralized two-stage coalition formation algorithms and particle swarm optimization were used to make a coalition of UAVs destroy the target. In [23] and [24], particle swarm optimization and its hybrid one with genetic algorithm were used to solve optimization problems with a non-linear objective function. Chen *et al.* studied cooperative area reconnaissance for multi-UAV in dynamic environment with optimum efficiency ensuring real-time application. [25] In their study, model predictive control and particle swarm optimization were used to control the UAVs for static and mobile threat avoidance while performing reconnaissance mission. However, these optimization-based approaches are computationally intensive and requires heuristic choice of a termination criterion to guarantee a convergence time and therefore is yet difficult to apply for real-time operations.

The force-field approach, or potential-field approach, assumes virtual fields around obstacles. Virtual attractive or repulsive forces created by these fields are used to generate collision avoidance maneuvers.[26-29] However, local minima may exist in the force field and cannot be easily addressed. Koren *et al.* presented inherent problems of potential field methods [30] as : oscillation in a high-speed real-time system and trap situations due to local minima. Paul *et al.* and Chen

J. Seo is with Defense Industry Technology Center, Agency for Defense Development, Seoul, Korea. (e-mail: sjb@add.re.kr)

Y. Kim is with Institute of Advanced Aerospace Technology, Department of Mechanical and Aerospace Engineering, Seoul National University, Seoul 151-744, Korea. (e-mail: ydkim@snu.ac.kr)

S. Kim is with Deptartment of Aerospace Engineering, Chungnam National University, Daejeon, Korea. (e-mail: skkim@cnu.ac.kr)

A. Tsourdos is with Deptartment of Informatics and Sensor, Cranfield University, Shrivenham, UK. (e-mail: a.tsourdos@cranfield.ac.uk)

Manuscript received

et al. found similar local minima problems when using an extended artificial potential field for formation flight of UAVs. [31], [32] The local minima was related with a length of time step and force gradient.

The sense-and-avoid approach, which is essentiallysimilar to a pilot's behavior in a manned aircraft, prevents a collision by changing the direction of travel of the aircraft away from the obstacle. The simplicity of the sense-and-avoid approach results in low computational requirements and short response times. The sense-and-avoid approach is more advantageous for UAVs than for manned aircraft, because UAVs usually have low-quality sensors for obstacle detection. Hence, research on sense-and-avoid method for UAV has been initiated since the late 1990s Prats *et al.* reviewed regulations, recommended practices, and standards in sense-and-avoid methods for unmanned aircraft [33]. Chakravarthy and Ghose proposed a collision-cone approach for collision detection and avoidance between irregularly shaped moving objects. The collision-cone approach can be effectively used to examine a condition of the collision between a robot and a moving obstacle [34]. Goss *et al.* considered a collision avoidance problem between two aircraft in a three dimensional environment using a combination of a geometric approach and a collision cone approach, and they proposed a guidance law based on the collision-cone approach [35]. In [36], a minimum-effort guidance law was developed to guide a UAV to a waypoint while avoiding multiple obstacles using the collision-cone approach. A two dimensional passive vision system and an extended Kalman filter were used to estimate the positions of the obstacles.

Considerable research has been devoted to making collision-cone guidance methods more practical for UAVs. Choi *et al.* proposed a vision-based collision avoidance system for a UAV using a single sensor [37]. Portilla *et al.* performed a feasibility study for a collision avoidance algorithm compatible with the Traffic Alert and Collision Avoidance System (TCAS II) used in manned aircraft [38]. Fasano *et al.* presented a fully autonomous multi-sensor anti-collision system for UAVs. This study used the collision geometry to detect and avoid obstacles. The UAVs were able to generate feasible trajectories in real time [39]. Shin *et al.* studied differential geometry for UAV conflict detection and resolution (CDR) and developed a guidance law to avoid collisions that included the physical and operational constraints of the vehicles [40]. White *et al.* investigated the use of differential geometry for UAV collision avoidance. This approach produces constant-curvature evasion maneuvers [41]. In [42], the collision cone approach was used to predict potential collisions between a UAVand an obstacle and, if necessary, compute a new direction to avoid the obstacle. The authors extended the algorithm to non-cooperative environments. Lalish and Morgansen investigated a reactive and distributed algorithm to guarantee that all UAVs avoid collisions while tracking their respective commands. A robustness analysis was performed to account for delays and actuator limits [43].

On the other hand, formation flight consisting of multiple UAVs has been continuously investigated with the topic of mission assignment or task assignment for path planning.[44-46] Information delivery and communication process among the vehicles are also important issues in formation flight.[47-49] However, the problem for a single UAV with static or dynamic obstacles has been mainly studied.[50-52] Especially, there are few results on collision avoidance for multiple-UAV formation with a specified geometry. It is reported in the literature to apply collision avoidance via a geometric strategy for formation regrouping, [53] and to generate paths using 'well clear volume' to avoid intruder via sense-and-avoid approach. [54]

This study proposes a collision-cone approach that includes dynamic constraints and a collision-avoidance envelope.A simple algorithm with low computational requirements is obtained by expanding the collision-cone approach to formations of UAVs. The proposed strategies can cope with pop-up obstacles promptly, because it can determine the avoidance direction based on the line-of-sight vector. As a result, local-minima, which is one of the problems in force-field approach, can be prevented, and each UAV can decide avoidance path instantaneously without an iteration or update process to obtain the collision avoidance direction. Also, the proposed algorithm can calculate the numerical index for collision avoidance, when UAVs select their ways of the avoidance against the obstacle.

Collision avoidance and formation management strategies proposed in this study also uses the result derived from a single calculation method to decide the next maneuver. The previous research have a weakness in that they do not deal with the possibility of formation keeping when UAVs avoid the collision. Instead, the proposed strategy suggests better direction to avoid the collision while maintaining the formation, because it considers a margin when UAVs avoid collision and simultaneously decides whether or not the specified formation can be maintained using this margin. To determine the feasibility of the proposed algorithm, simulations of various scenarios were conducted using a point-mass UAV model with dynamic constraints. The results of the numerical simulations show good performance for coordinated collision avoidance by multiple UAVs. Therefore, the proposed algorithm can be effective in practical UAV operations.

The paper is organized as follows. Section II introduces definitions and assumptions for the formulation of the collision avoidance problem. Section III presents a collision avoidance algorithm based on geometry. In Section III, the guidance law is analyzed using Lyapunov theory, and an envelope for successful collision avoidance is introduced. Then, a formation management strategy is developed using the collision avoidance envelope. Section IV presents the results of numerical simulations to demonstrate the performance of the collision avoidance and formation management strategies. Concluding remarks are presented in Section V.

II. Fundamentals of Collision Avoidance

A. *Definitions and Assumptions*

This section provides definitions of collisions and obstacle detection.

Definition 2.1 (Collision). A collision between a UAV

and an obstacle is defined as follows:

$$\| \mathbf{r}_u - \mathbf{r}_o \| < d_C \tag{1}$$

where $\mathbf{r}_u$ and $\mathbf{r}_o$ denote the position vectors of the UAV and the obstacle, respectively, and d_C is the collision radius.

◇

Definition 2.2 (Detection). An obstacle is detected by a UAV when the following condition is satisfied:

$$\| \mathbf{r}_u - \mathbf{r}_o \| < d_{RG} \tag{2}$$

where d_{RG} denotes a specified detection radius, which can be derived from the performance of the on-board sensor system.

◇

The following assumptions from [39], [42], and [45] were used in this study:

Assumption 1 : All UAVs and all obstacles have constant ground speeds, and the direction of the velocity vector of an obstacle is constant.

Assumption 2 : Each UAV acquires its own velocity and position vectors using an on-board sensor system, and all UAVs communicate with each other without information loss.

By sharing information, the relative distances and velocities between the UAVs can be computed.

B. Equations of Motion

Let us consider the following three-dimensional point-mass model of a UAV:

$$\begin{aligned}
\dot{x} &= v\cos\gamma\cos\psi \\
\dot{y} &= v\cos\gamma\sin\psi \\
\dot{z} &= v\sin\gamma
\end{aligned} \tag{3}$$

where γ and ψ are the flight path angle and the heading angle, respectively. Note that the motion in the horizontal plane is decoupled from that in the vertical plane. It is assumed that the closed-loop aircraft dynamics can be modeled as a first-order system with flight path angle commands γ_c and heading angle commands ψ_c as follows.

$$\begin{aligned}
\dot{\gamma} &= -\frac{1}{\tau_\gamma}\gamma + \frac{1}{\tau_\gamma}\gamma_c \\
\dot{\psi} &= -\frac{1}{\tau_\psi}\psi + \frac{1}{\tau_\psi}\psi_c
\end{aligned} \tag{4}$$

where τ_γ and τ_ψ are time constants.

The speed v of the UAV can be computed as

$$v = \sqrt{v_H^2 + v_V^2} \tag{5}$$

where v_H and v_V are the horizontal velocity and the vertical velocity of the UAV, respectively, which can be computed as

$$\begin{aligned}
v_H &= v\cos\gamma \\
v_V &= v\sin\gamma.
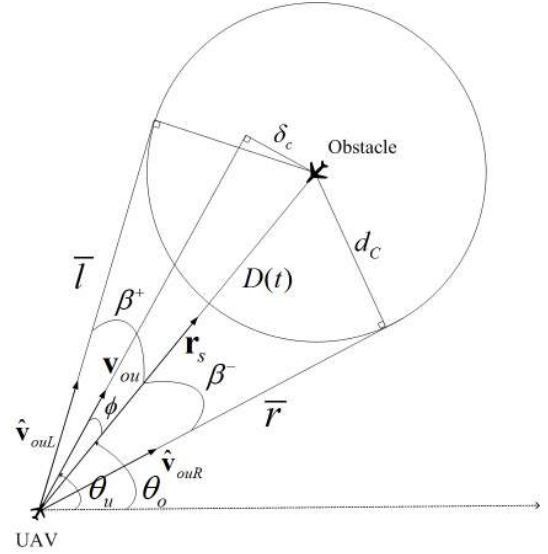\end{aligned} \tag{6}$$

Fig. 1. Single obstacle avoidance with a geometric guidance law.

III. COLLISION AVOIDANCE GUIDANCE

A. Collision Avoidance based on Geometry

1) Single obstacle:

To avoid a collision between a UAV and an obstacle, the UAV should not violate the collision criterion in Eq. (1). Based on the relative geometry in the two-dimensional plane, there exist two options for the UAV to avoid the obstacle.

Assume that a UAV encounters an obstacle with a collision radius d_C, as shown in Fig. 1. In Fig. 1, the subscripts o and u denote the obstacle and the UAV, respectively. For example, $\mathbf{v}_u$ and $\mathbf{v}_o$ denote the velocities of the UAV and the obstacle, respectively. The vector $\mathbf{v}_{ou}$ denotes the relative velocity of the obstacle with respect to the UAV. From the current position of the UAV, two lines can be drawn that are tangent to the circle defined by the collision radius, the line $\bar{l}$, which is the tangent on the left side of the obstacle, and the line $\bar{r}$, which is tangent on the right side of the obstacle. Either of these paths could be chosen as the direction for the UAV velocity vector. We denote the two possible velocity vectors as $\hat{\mathbf{v}}_{ouL}$ and $\hat{\mathbf{v}}_{ouR}$. Using differential geometry, a collision avoidance law for a UAV [40] can be obtained using the angles between the UAV-obstacle relative velocity vector and the tangent lines. The desired relative velocity, $\hat{\mathbf{v}}_{ou}$, can be determined as follows:

$$\hat{\mathbf{v}}_{ou} = \begin{cases} \hat{\mathbf{v}}_{ouL} & \text{if } \theta_o \leq \theta_u \leq \theta_o + \beta^+ \\ \hat{\mathbf{v}}_{ouR} & \text{if } \theta_o + \beta^- \leq \theta_u < \theta_o \\ \mathbf{v}_{ou} \text{ (No change)} & \text{if } \theta_u < \theta_o + \beta^- \text{ or } \theta_o + \beta^+ > \theta_u \end{cases} \tag{7}$$

where θ_o and θ_u are the angles of the line-of-sight vector between the obstacle and the UAV and the velocity vector of the UAV in the inertial frame, respectively, with respect to the x-axis and β^+ ($\beta^+ > 0$) and β^- ($\beta^- < 0$) are the angles of the tangent line vectors $\bar{l}$ and $\bar{r}$ with respect to the line-of-sight vector $\mathbf{r}_s$. To choose between $\bar{l}$ and $\bar{r}$ to avoid a collision, a collision detection angle is defined.

Definition 3.1 (Collision Detection Angle). For $\mathbf{r}_s \neq 0$ and $\mathbf{v}_{ou} \neq 0$, the collision detection angle ϕ is defined by the line-of-sight vector $\mathbf{r}_s$ and the relative velocity vector $\mathbf{v}_{ou}$ as follows:

$$\phi = \begin{cases} \cos^{-1}\left[\frac{\mathbf{r}_s \cdot \mathbf{v}_{ou}}{|\mathbf{r}_s|\,|\mathbf{V}_{ou}|}\right] \\ \phi \triangleq \pi/2 & \text{for } \mathbf{r}_s = 0, \mathbf{v}_{ou} = 0 \end{cases} \tag{8}$$

◇

Definition 3.2 (Closest Point of Approach). The closest point of approach (CPA) δ_c of the UAV to the obstacle can be expressed using the relative geometry shown in Fig. 1 as follows:

$$\delta_c = |\mathbf{r}_s| \sin\phi \tag{9}$$

where ϕ is the collision detection angle.

◇

The UAV has two options for changing direction to avoid a collision: (i) the vector $\bar{l}$; i.e., a turn to the left, or (ii) the vector $\bar{r}$; i.e., a turn to the right. For each direction, the turn angles σ_L and σ_R can be computed using β and ϕ as follows:

$$\begin{aligned} \sigma_L &= \beta^+ - \phi \quad \text{(left turn angle)} \\ \sigma_R &= \beta^- - \phi \quad \text{(right turn angle)} \end{aligned} \tag{10}$$

If $\beta^- < \phi < \beta^+$, then the smaller of σ_L and σ_R is chosen for obstacle avoidance so that the minimum amount of effort, as measured by the magnitude of the required turn angle σ, becomes the criterion in choosing the change of direction; i.e.,

$$\sigma = \begin{cases} |\sigma_L|, & \text{if } |\sigma_L| \leq |\sigma_R| \quad \text{(left turn)} \\ -|\sigma_R|, & \text{if } |\sigma_L| > |\sigma_R| \quad \text{(right turn)} \end{cases} \tag{11}$$

If $\beta^+ < \phi$ or $\beta^- > \phi$, then $\sigma = 0$, in which case no action is required.

In summary, the strategy for avoiding a collision with a single obstacle is to align the relative velocity vector with one of the tangent line vectors. However, multiple obstacles may be simultaneously recognized in many cases, even they have overlapped collision area. In order to cope with such a case, additional guidance is remarked in following section.

2) Multiple obstacles:

To avoid collisions with multiple obstacles, the new direction should be calculated considering all of the obstacles with which there is a possibility of a collision. Let us assume that a UAV can detect all obstacles within the range of its sensors. Two cases, shown in Fig. 2, can be considered. Figure 2(a) illustrates the case in which a near-field obstacle is located on the left of a far-field obstacle, and Fig. 2(b) shows the reverse case. The collision avoidance direction can be derived from the geometry, as will be explained in the following.

Let us first consider $\mathbf{v}_{ou1}$. From Fig. 2, the following conditions for the angles of the relative velocity vectors are obtained:

$$\begin{aligned} &\text{Case 1}: \angle\hat{\mathbf{v}}_{ouL1} > \angle\hat{\mathbf{v}}_{ouL2} > \angle\hat{\mathbf{v}}_{ouR1} \\ &\text{Case 2}: \angle\hat{\mathbf{v}}_{ouL1} > \angle\hat{\mathbf{v}}_{ouR2} > \angle\hat{\mathbf{v}}_{ouR1} \end{aligned} \tag{12}$$
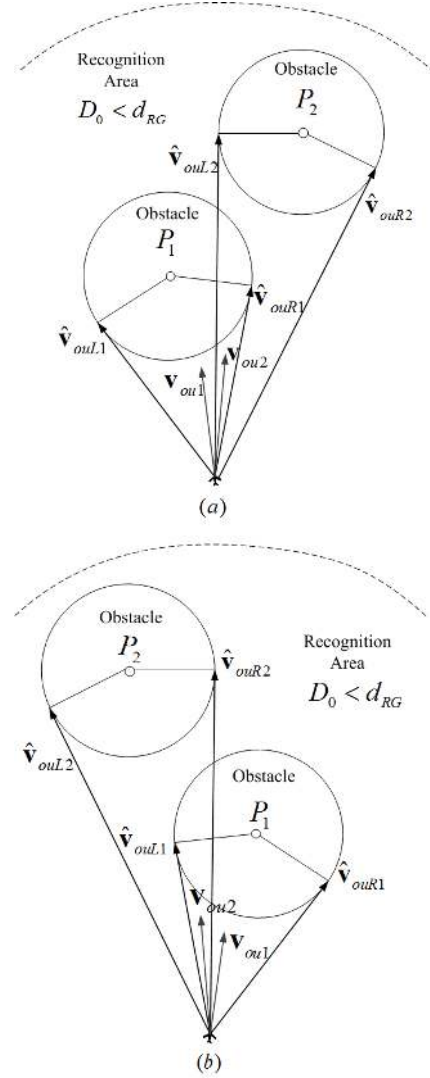

Fig. 2. Collision avoidance for multiple obstacles or multiple-obstacle collision avoidance. (a) Case 1 : obstacle 1 is on the leftside of obstacle 2; (b) Case 2 : obstacle 1 is on the rightside of obstacle 2.

For both cases, β^+ and β^- can be obtained as follows:

$$\begin{aligned} \beta^+ &= \max(\angle\hat{\mathbf{v}}_{ouL1}, \angle\hat{\mathbf{v}}_{ouL2}) \\ \beta^- &= -\max(|\angle\hat{\mathbf{v}}_{ouR1}|, |\angle\hat{\mathbf{v}}_{ouR2}|) \end{aligned} \tag{13}$$

The computed angles β^+ and β^- are used to obtain $(\sigma_{L1}, \sigma_{R1})$ and σ_1 as in the single-obstacle case:

$$\begin{aligned} \sigma_{L1} &= \beta^+ - \phi_1 \quad \text{(left turning angle)} \\ \sigma_{R1} &= \beta^- - \phi_1 \quad \text{(right turning angle)} \end{aligned} \tag{14}$$

$$\sigma_1 = \begin{cases} |\sigma_{L1}|, & \text{if } |\sigma_{L1}| \leq |\sigma_{R1}| \\ -|\sigma_{R1}|, & \text{if } |\sigma_{L1}| > |\sigma_{R1}| \end{cases}$$

where ϕ_1 is the collision detection angle for the obstacle 1. Similarly, for $\mathbf{v}_{ou2}$, the following angular conditions are obtained.:

$$\begin{aligned} &\text{Case 1}: \angle\hat{\mathbf{v}}_{ouL2} > \angle\hat{\mathbf{v}}_{ouR1} > \angle\hat{\mathbf{v}}_{ouR2} \\ &\text{Case 2}: \angle\hat{\mathbf{v}}_{ouL2} > \angle\hat{\mathbf{v}}_{ouL1} > \angle\hat{\mathbf{v}}_{ouR2} \end{aligned} \tag{15}$$

For both cases, β^+ and β^- can be obtained as follows:

$$\begin{aligned} \beta^+ &= \max(\angle\hat{\mathbf{v}}_{ouL1}, \angle\hat{\mathbf{v}}_{ouL2}) \\ \beta^- &= -\max(|\angle\hat{\mathbf{v}}_{ouR1}|, |\angle\hat{\mathbf{v}}_{ouR2}|) \end{aligned} \tag{16}$$

Similarly, the turn angles $(\sigma_{L2}, \sigma_{R2})$ and σ_2 are chosen as follows:

$$
\begin{aligned}
\sigma_{L2} &= \beta^+ - \phi_2 \quad \text{(left turning angle)} \\
\sigma_{R2} &= \beta^- - \phi_2 \quad \text{(right turning angle)}
\end{aligned} \tag{17}
$$

$$
\sigma_2 = \begin{cases} |\sigma_{L2}|, & \text{if } |\sigma_{L2}| \leq |\sigma_{R2}| \\ -|\sigma_{R2}|, & \text{if } |\sigma_{L2}| > |\sigma_{R2}| \end{cases}
$$

where ϕ_2 is the collision detection angle for obstacle 2. Finally, the collision avoidance maneuver for multiple obstacles is determined by considering the geometry of obstacles 1 and 2 as follows:

$$
\sigma = \max(|\sigma_1|, |\sigma_2|) \tag{18}
$$

Note that if σ_1 or σ_2 from Eq. (18) is initially less than zero, then $\sigma = -|\sigma|$. It can be shown that choosing the maximum angle σ among the angles corresponding to each obstacle will guarantee collision avoidance. In Fig. 2, only two obstacles are considered; however, additional obstacles can be included in the same manner by choosing the outermost velocity vector.

Also, collision avoidance maneuvers can also be derived using the flight path angle γ in the vertical plane. $\mathbf{v}_i$ is the relative velocity vector of the UAV with respect to obstacle i. This vector can be projected onto the XY-plane to determine horizontal maneuvers $(\mathbf{v}_{iXY})$ and onto the XZ-plane to determine vertical maneuvers $(\mathbf{v}_{iXZ})$, respectively, where $\mathbf{v}_{iXY}$ and $\mathbf{v}_{iXZ}$ correspond to the vector $\mathbf{v}_{oui}$ from Fig. 2 used to calculate σ in the XY-plane and the XZ-plane, respectively.

3) Algorithm for collision avoidance:
Figure 3 shows a flow chart of the collision avoidance algorithm. Before choosing the direction for obstacle avoidance, potential collisions must first be identified. It should be noted that in Eqs. (12)-(18) the UAV calculates the relative vectors and the collision avoidance direction using the information on all of the obstacles located in the space defined by d_{RG}. This process may increase the computational load. Therefore, the following additional conditions are considered for collision avoidance:

$$
\mathbf{r}_s \cdot \mathbf{v}_{ou} \geq 0 \tag{19}
$$

$$
D(t) \sin \phi < d_C \tag{20}
$$

where $D(t)$ is the distance between the UAV and the obstacle and $\mathbf{r}_s$ and $\mathbf{v}_{ou}$ are the line-of-sight vector and the relative velocity vector of the obstacle, respectively. Equation (19) specifies that only the obstacles located within the angular range of $\pm\frac{\pi}{2}$ are considered. Hence, although an obstacle may be detected within d_{RG}, no evasive action is required if the collision detection angle ϕ is beyond $\pm\frac{\pi}{2}$. As mentioned in the previous section, the term $D(t) \sin \phi$ in Eq. (20) is the magnitude of the CPA between the obstacle and the UAV at the time the potential collision is detected. If both conditions in Eqs. (19) and (20) are satisfied, the avoidance maneuver is performed.

For multiple obstacles, the completion of a collision avoidance maneuver must be identified to guide the UAV to the original goal point. The conflict detection algorithm
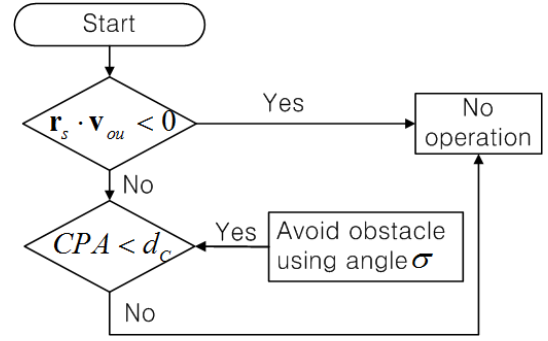

Fig. 3. Block diagram of collision avoidance logic.

also determines the completion of the collision avoidance maneuver. The following definition is used to determine when the collision avoidance maneuver has been completed.

Definition 3.3. (Completion of Collision Avoidance). A collision avoidance maneuver is complete if the value of the projection of $\mathbf{r}_s(\mathbf{r}_s \neq 0)$ onto $\mathbf{v}_{ou}(\mathbf{v}_{ou} \neq 0)$ is less than zero. The projection of $\mathbf{r}_s$ onto $\mathbf{v}_{ou}$ is defined as

$$
\begin{aligned}
Proj_{\mathbf{v}_{ou}} \mathbf{r}_s &= \alpha \mathbf{v}_{ou} \\
&= \frac{\|\mathbf{r}_s\| \cdot \|\mathbf{v}_{ou}\| \cos \phi}{\|\mathbf{v}_{ou}\|^2} \mathbf{v}_{ou}
\end{aligned} \tag{21}
$$

where α is a scalar.
When the collision has been successfully avoided, the relative velocity vector $\mathbf{v}_{ou}$ is perpendicular to the line-of-sight vector $\mathbf{r}_s$ and the magnitude of the collision detection angle ϕ reaches $\frac{\pi}{2}$. The angle ϕ increases and becomes an obtuse angle at the moment of completion. According to the definition in Eq. (21), if $\cos \phi < 0$, then the collision avoidance maneuver is complete.

◇

B. *Design of a Guidance Law for Collision Avoidance*

In this section, a guidance law is derived to give the UAV the desired relative velocity vector. Figure 1 shows the geometry for avoiding a collision with an obstacle using the line-of-sight vector. The change in direction of the UAV can be determined by evaluating ϕ and β. Let us analyze the stability of the guidance law in the following.
Consider the following candidate Lyapunov function:

$$
V = \frac{1}{2} \gamma_e^2 + \frac{1}{2} \psi_e^2 \tag{22}
$$

Using Eq. (4), the heading and flight path angle commands can be obtained:

$$
\begin{aligned}
u_\gamma &= \gamma - k_\gamma \tau_\gamma \gamma_e = \gamma - k_\gamma \tau_\gamma (\gamma - \hat{\gamma}) \\
u_\psi &= \psi - k_\psi \tau_\psi \psi_e = \psi - k_\psi \tau_\psi (\psi - \hat{\psi})
\end{aligned} \tag{23}
$$

where the constants k_γ and $k_\psi 0$
have positive values. Substituting Eq. (23) into Eq. (22) and then differentiating yields

$$
\begin{aligned}
\dot{V} &= \dot{\gamma}_e \gamma_e + \dot{\psi}_e \psi_e \\
&= \dot{\gamma}_e (\gamma - \hat{\gamma}) + \dot{\psi}_e (\psi - \hat{\psi})
\end{aligned} \tag{24}
$$

Substituting Eq. (4) in Eq. (24) gives

$$\dot{V} = \frac{(u_\gamma - \gamma)}{\tau_\gamma}(\gamma - \hat{\gamma}) + \frac{(u_\psi - \psi)}{\tau_\psi}(\psi - \hat{\psi})$$
$$= -k_\gamma(\gamma - \hat{\gamma})^2 - k_\psi(\psi - \hat{\psi})^2 \le 0 \quad (25)$$

Therefore, the states γ, and ψ converge to the desired states $\hat{\gamma}$ and $\hat{\psi}$ asymptotically by the Lyapunov stability theorem.

C. Guidance for Collision Avoidance in Constrained Envelope

1) Envelope for successful avoidance:

Using the guidance command derived in section III-B, collision avoidance is guaranteed regardless of the relative distance between an obstacle and a UAV if the turn rate of the UAV is unbounded, which is not true in reality. The TCAS (Traffic Alert and Collision Avoidance System), which assists in preventing collisions between manned aircraft, employs various information such as air traffic control practices and limits on aircraft performance. The latest version, TCAS II [56], provides traffic advisories (TAs) and resolution advisories (RAs) in the vertical dimension to either increase or maintain the vertical separation between aircraft. For vertical maneuvers, the climb rate and other limits on the dynamics of the vehicle should be considered.

If there is an angular rate limit in the UAV dynamics, it may be impossible to avoid collision using Eq. (23). Therefore, it is necessary to determine whether the collision is avoidable using the proposed guidance law. Additionally, the avoidance path should be chosen in accordance with the limits of the envelope. This section investigates the effect of these constraints on the angular rate limits of the UAV in collision avoidance. The following definitions characterize the envelope for successful collision avoidance.

Definition 3.4. (Collision Avoidance Margin). S is a scalar function of the relative geometry between a UAV and an obstacle and is defined as follows:

$$S(\mathbf{X}) = D(t)\cos\phi - \sqrt{d_C^2 - D(t)^2 \sin^2\phi} - |\mathbf{v}_{ou}| \cdot \frac{\sin^{-1}\left(\frac{d_C}{D(t)}\right) - \left|\cos^{-1}\left(\frac{\mathbf{r}_s \cdot \mathbf{v}_{ou}}{|\mathbf{r}_s|\,|\mathbf{v}_{ou}|}\right)\right|}{r_{lim}}$$
$$(26)$$

where $\mathbf{X} = [\mathbf{v}_{ou}, \ \mathbf{r}_s]$, $D(t)$ is the current relative distance between the UAV and the obstacle, ϕ is the collision detection angle, and r_{lim} is the angular rate limit.

$\diamond$

Definition 3.5. (Envelope for Collision Avoidance). When a UAV detects an obstacle, an envelope for successful collision avoidance can be defined with the collision avoidance index S:

Let $\mathbf{A} = \{\mathbf{X} \in \mathbb{R}^{6\times1} \mid S(\mathbf{X}) > 0\}$. If $\mathbf{X} \in \mathbf{A}$, then the obstacle is avoidable by the UAV at a distance $D(t^*)$, where t^* denotes the time at which the conflict is detected.

$\diamond$

From Fig. 4 it can be observed that the direction of the relative velocity vector should be changed by the angle σ to avoid the obstacle. The yaw rate is limited to $\pm r_{lim}$ ($r_{lim} > 0$), so
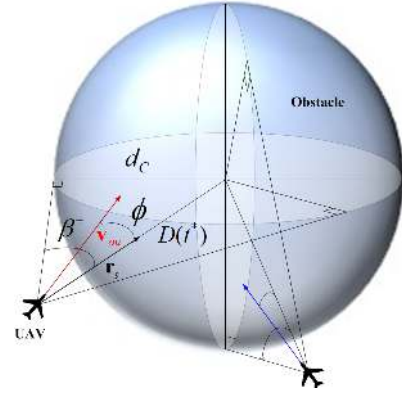
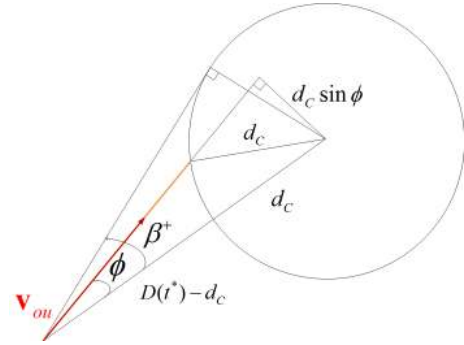

Fig. 4. Envelope for successful collision avoidance.

Fig. 5. Clearance distance at the time of detection.

the maneuver must be completed in an interval of time T_{yaw}, which will be derived next.

Consider the case $\beta = \beta^+$ ($\beta^+ > 0$), in which case the UAV turns left. Then, T_{yaw} can be computed as

$$T_{yaw} = \frac{|\sigma|}{r_{lim}} = \frac{\beta^+ - |\phi|}{r_{lim}} \quad (27)$$

Thus, T_{yaw} seconds are required to perform the turn, so the turn must begin at least this far in advance to avoid a collision. At the time of detection, t^*, a required clearance distance between the UAV and the obstacle can be expressed using the collision radius and the collision detection angle, as shown in Fig. 5. Then, the distance between the UAV and the obstacle should satisfy the following condition:

$$D(t^*)\cos\phi - \sqrt{d_C^2 - D(t^*)^2 \sin^2\phi} > |\mathbf{v}_{ou}| \cdot \frac{\beta^+ - |\phi|}{r_{lim}} \quad (28)$$

From the geometry shown in Fig. 4, β^+ can be computed as

$$\beta^+ = \sin^{-1}\left(\frac{d_C}{D(t^*)}\right) \quad (29)$$

Substituting Eq. (29) and the collision detection angle in Eq. (8) into Eq. (28), the minimum required clearance distance for the collision to be avoided can be obtained:

$$D(t^*)\cos\phi - \sqrt{d_C^2 - D(t^*)^2 \sin^2\phi} > |\mathbf{v}_{ou}| \cdot \frac{\sin^{-1}\left(\frac{d_C}{D(t^*)}\right) - \left|\cos^{-1}\left(\frac{\mathbf{r}_s \cdot \mathbf{v}_{ou}}{|\mathbf{r}_s|\,|\mathbf{v}_{ou}|}\right)\right|}{r_{lim}}$$
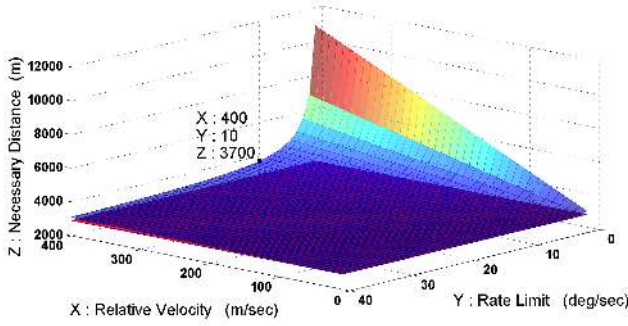$$(30)$$

Fig. 6. Envelope for successful collision avoidance when $\sigma = 20$ (*deg*).

Next, let us consider the case $\beta = \beta^-$ ($\beta^- < 0$), in which case the UAV turns right. In this case, T_{yaw} can be computed as

$$T_{yaw} = \frac{|\sigma|}{r_{lim}} = \frac{|\beta^-| - |\phi|}{r_{lim}} \tag{31}$$

where $\beta^- < \phi < 0$.

From the geometry shown in Fig. 4, β^- can be computed as

$$\beta^- = -\beta^+ = -\sin^{-1}\left(\frac{d_C}{D(t^*)}\right) \tag{32}$$

Similarly, a minimum clearance distance can be derived for the $\beta = \beta^-$ case. The distance between the UAV and the obstacle must satisfy the following condition at the time the conflict is detected t^* to avoid a collision.

$$D(t^*)\cos\phi - \sqrt{d_C^2 - D(t^*)^2 \sin^2\phi} - |\mathbf{v}_{ou}| \cdot \frac{\sin^{-1}\left(\frac{d_C}{D(t^*)}\right) - \left|\cos^{-1}\left(\frac{\mathbf{r}_s \cdot \mathbf{v}_{ou}}{|\mathbf{r}_s| |\mathbf{v}_{ou}|}\right)\right|}{r_{lim}} > 0 \tag{33}$$

A similar condition can be derived for the clearance distance for a vertical maneuver:

$$D(t^*)\cos\phi - \sqrt{d_C^2 - D(t^*)^2 \sin^2\phi} - |\mathbf{v}_{ou}| \cdot \frac{\sin^{-1}\left(\frac{d_C}{D(t^*)}\right) - \left|\cos^{-1}\left(\frac{\mathbf{r}_s \cdot \mathbf{v}_{ou}}{|\mathbf{r}_s| |\mathbf{v}_{ou}|}\right)\right|}{q_{lim}} > 0 \tag{34}$$

where q_{lim} is the pitch rate limit.

$\diamond$

Note that the detection range d_{RG} and the angular rate limits r_{lim} and q_{lim} are important constraints that determine whether a collision can successfully be avoided. Therefore, at the moment that an obstacle is detected, i.e., $D(t^*) = d_{RG}$, the following conditions are required for successful collision avoidance.

- For horizontal maneuvers :

$$d_{RG}\cos\phi - \sqrt{d_C^2 - d_{RG}^2 \sin^2\phi} - |\mathbf{v}_{ou}| \cdot \frac{\sin^{-1}\left(\frac{d_C}{d_{RG}}\right) - \left|\cos^{-1}\left(\frac{\mathbf{r}_s \cdot \mathbf{v}_{ou}}{|\mathbf{r}_s| |\mathbf{v}_{ou}|}\right)\right|}{r_{lim}} > 0 \tag{35}$$

- For vertical maneuvers :

$$d_{RG}\cos\phi - \sqrt{d_C^2 - d_{RG}^2 \sin^2\phi} - |\mathbf{v}_{ou}| \cdot \frac{\sin^{-1}\left(\frac{d_C}{d_{RG}}\right) - \left|\cos^{-1}\left(\frac{\mathbf{r}_s \cdot \mathbf{v}_{ou}}{|\mathbf{r}_s| |\mathbf{v}_{ou}|}\right)\right|}{q_{lim}} > 0 \tag{36}$$

A simple example is presented to demonstrate the use of the envelope for collision avoidance. Figure 6 shows the envelope for successful collision avoidance for a collision radius $d_C = 2,900m$ and $\sigma = 20$ degree. For an angular rate limit of 10 deg/sec and a relative velocity between the UAV and the obstacle of 400 m/sec, the necessary clearance distance should be greater than 3,700 m to guarantee avoidance, as shown in Fig. 6. Note that the distance d_C is chosen as the lower boundary.

The condition for a UAV to successfully avoid a collision can be obtained from Eq. (26). Using the collision avoidance margin S, it is possible to determine whether a collision with an obstacle is avoidable or not at the time of detection. This property can also be used for multiple conflicts.

2) Collision avoidance for multiple UAVs and envelope analysis:
As discussed in the previous section, collision avoidance can be achieved using the angular rate limit and the relative distance between the UAV and an obstacle when the UAV detects the obstacle. Using the collision avoidance margin S, the UAV can determine whether a collision is avoidable with the given angular rate limit in either the horizontal or vertical planes. This property can serve as the basis for selecting the horizontal and/or vertical plane for maneuvering. In other words, each UAV in a formation can predict the feasibility of collision avoidance, and the avoidance path can be chosen. Note the following specific observations on the choice of the plane and the direction to avoid a collision using the collision avoidance margin S.

Remark 3.1: (Choice of collision avoidance plane) Each UAV has collision avoidance margins in the horizontal and vertical planes. To determine the plane for maneuvering, a plane with a negative value of S is excluded. A negative value of S indicates that the predicted minimum distance between the UAV and the obstacle is less than the collision radius d_C and therefore a collision is unavoidable.

Let us consider cases in which a UAV in formation can avoid an obstacle by maneuvering in at least one plane. Then, one of the following three collision avoidance strategies can be chosen:

- Maneuver only in the horizontal plane.
- Maneuver only in the vertical plane.
- Maneuver in both the horizontal and vertical planes.

If both planes are used for collision avoidance with multiple UAVs, it is difficult to specify the proper formation in three-dimensions. Additionally, the formation may be distorted. One of main objectives of this study is to maintain the formation whenever possible without a collision. Therefore, priority is given to the horizontal plane in the third case when both planes are possible. This policy also prevents the consumption of additional energy required for altitude changes.

$\diamond$

Remark 3.2: (Choice of collision avoidance direction) Applying the strategy in Remark 3.1, the UAV can find an available plane to avoid a collision. The UAV can choose the direction in the selected plane from the angle between the relative velocity
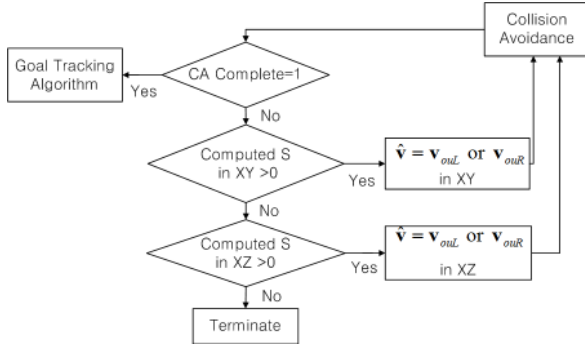
Fig. 7. A flow chart of collision avoidance strategy with the constraint envelope.

vector and the line-of-sight vector, which was explained in section III-A. In summary, turning left or right is possible in the horizontal plane, and either pitching up (positive) or down (negative) is possible in the vertical plane. And, for a symmetric case which has the same value of S, priority is given to the turning right direction in horizontal plane and to the pitching up direction in the vertical plane, respectively. Note that goal-point tracking is conducted in the plane in which an avoidance command is not applied.

◇

Figure 7 shows a flow chart of the collision avoidance strategy after an obstacle is detected. First, the UAV scans for obstacles. If the UAV does not detect any obstacles, then goal-point tracking is performed in both planes. If an obstacle is detected and cannot be avoided in the horizontal plane, then the UAV performs a collision avoidance maneuver using a flight path angle command (i.e., the vertical plane) and continues goal-point tracking in the horizontal plane using heading angle commands, as discussed in Remark 3.2.

D. Formation Keeping and Splitting

1) Strategy for formation keeping and splitting:
This section discusses a formation keeping and splitting strategy based on the collision avoidance scheme. Let us consider a situation in which n UAVs in formation encounter an obstacle P, and each UAV detects the obstacle P within the detection distance. Each UAV calculates the values of the collision avoidance margin S in both the horizontal and vertical planes using Eq. (26):

$$
\begin{array}{lll}
S_{(1,P,H)}, & S_{(1,P,V)} & : & \text{S values of UAV 1} \\
S_{(2,P,H)}, & S_{(2,P,V)} & : & \text{S values of UAV 2} \\
S_{(3,P,H)}, & S_{(3,P,V)} & : & \text{S values of UAV 3} \\
& \vdots & & \\
S_{(n,P,H)}, & S_{(n,P,V)} & : & \text{S values of UAV } n
\end{array} \tag{37}
$$

where $S_{(i,P,H)}$ denotes the value of S assuming that UAV i can avoid the obstacle P in the horizontal plane.

Next, let us consider a case in which a formation of UAVs cannot avoid an obstacle as a whole. In this case, each UAV can avoid the obstacle using an available plane, which can

be determined from the collision avoidance envelope given by Eq. (26). The following remark describes the method by which UAVs in a formation can be divided into several groups in a collision avoidance maneuver.

Remark 3.3 : (Sharing of avoidance commands). As mentioned in section III-C2, each UAV chooses the plane and the direction to avoid the obstacle. For the UAVs that have the same maneuver plane and direction, the avoidance command is shared for formation keeping during the collision avoidance maneuver. We define S_{minH} as the minimum value of S among those UAVs avoiding the obstacle P and having the same direction in the horizontal plane.

$$
S_{minH} = \min\{S_{(1,P,H)}, S_{(2,P,H)}, ..., S_{(n,P,H)}\} \tag{38}
$$

where $S_{(i,P,H)} > 0$ for $i = 1,..,n$ where each UAV has the same maneuver direction in the horizontal plane.
From Eq. (38), S_{minH} is the minimum S value among those UAVs having the same maneuver direction in the horizontal plane. For all UAVs having the same plane and the same direction, an identical command u_i can be chosen:

$$
u_i = \{\text{the input } u \text{ of UAV } i \mid S_{(i,P,H)} = S_{minH}\} \tag{39}
$$

Note that the collision avoidance margin S describes the magnitude of the required relative distance when the UAV avoids the obstacle with maximum effort. The UAV having the smallest value of S will require the greatest effort to avoid a collision. Because the same command is used by all of the UAVs with the same maneuvering plane and direction, the formation will be maintained while preventing collisions not only between the UAVs and the obstacle but also among the UAVs in the formation.

◇

In summary, for all UAVs that must avoid the obstacle using the horizontal plane and the same direction, the heading angle command is

$$
u_H = \{u_i \mid S_{(i,P,H)} = S_{minH}\}. \tag{40}
$$

Similarly, for all of the UAVs that must avoid the obstacle using the vertical plane and the same direction, the flight path angle command is

$$
u_V = \{u_i \mid S_{(i,P,V)} = S_{minV}\}. \tag{41}
$$

Note that for the UAVs having different maneuvering planes, the same command cannot be used. Additionally, for the UAVs having different maneuver directions, although they have the same maneuvering plane, the same command cannot be used. In these cases, each UAV should maneuver with its own command. This situation requires that the UAVs break formation, which will be discussed in the following section.

2) Condition for formation keeping and splitting:
In the previous section, the protocol of command sharing was introduced to avoid collisions while maintaining a formation. This section presents a condition to determine if multiple UAVs can maintain the formation during obstacle avoidance.
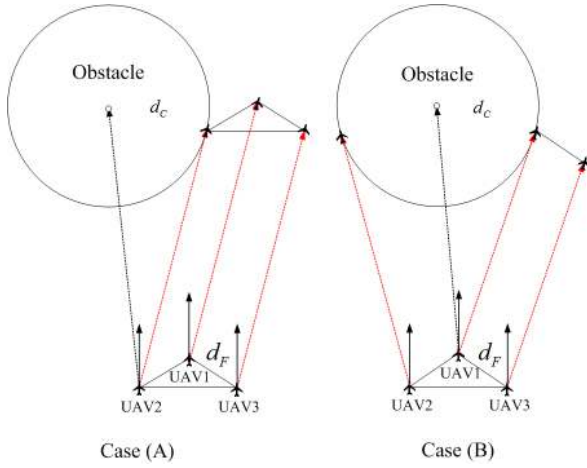
Fig. 8. Two cases avoidance for three UAVs in a triangular formation.

Fig. 9. Flowchart of the obstacle avoidance and formation-keeping algorithm for multiple UAVs.

Consider a formation consisting of three UAVs encountering a potential collision, as shown in Fig. 8. Without distinguishing left from right, there exist two possible cases: (A) a maneuver by the formation of three UAVs, and (B) different maneuvers by a single UAV and a formation of two UAVs.

- Case (A):

  In this case, all of the UAVs turn in the same direction according to the collision avoidance logic. The formation can be maintained by all of the UAVs if the highest required turn rate for collision avoidance among all of the UAVs (UAV 2) is possible.

  Because the condition for maintaining the formation is equivalent to the condition of the outermost UAV being capable of avoiding the collision, the collision avoidance margin can be expressed as follows

  $$S(\mathbf{X}) = d_{RG}\cos\phi - \sqrt{d_C^2 - d_{RG}^2\sin^2\phi} \qquad (42)$$
  $$- |\mathbf{v}_{ou}| \cdot \frac{\sin^{-1}\left(\frac{d_C}{d_{RG}}\right) - \left|\cos^{-1}\left(\frac{\mathbf{r}_s \cdot \mathbf{v}_{ou}}{|\mathbf{r}_s|\ |\mathbf{v}_{ou}|}\right)\right|}{r_{lim}} > 0$$
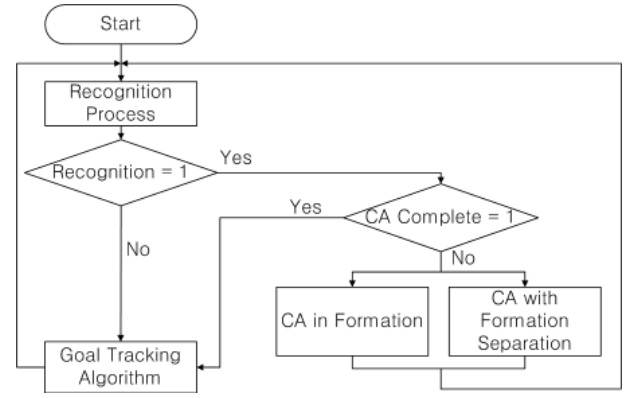
  where $\mathbf{X} = [\mathbf{v}_{ou},\ \mathbf{r}_s]$ is calculated from the state of the UAV that has the largest conflict detection angle in the formation.

- Case (B):

  In this case, one of UAVs must turn in a different direction based on the collision avoidance logic. As mentioned in Remark 3.3, the UAVs having the same maneuver direction can maintain the formation, and the UAV having a different maneuver direction should break formation. Consequently, the condition of sub-formation keeping is equivalent to the condition of successful collision avoidance by the UAV having the largest conflict detection angle, and the collision avoidance margin can be expressed as follows:

  $$S(\mathbf{X}) = d_{RG}\cos\phi - \sqrt{d_C^2 - d_{RG}^2\sin^2\phi} \qquad (43)$$
  $$- |\mathbf{v}_{ou}| \cdot \frac{\sin^{-1}\left(\frac{d_C}{d_{RG}}\right) - \left|\cos^{-1}\left(\frac{\mathbf{r}_s \cdot \mathbf{v}_{ou}}{|\mathbf{r}_s|\ |\mathbf{v}_{ou}|}\right)\right|}{r_{lim}} > 0$$

where $\mathbf{X} = [\mathbf{v}_{ou},\ \mathbf{r}_s]$ is calculated from the state of the UAV that has the largest conflict detection angle in the sub-formation.

Note that the condition for successful formation keeping can be obtained using the collision radius and the relative distance/velocity between the UAVs and the obstacle.

In summary, each UAV can decide which plane and direction to use to avoid the collision using the approach described in Remarks 3.1 and 3.2. Subsequently, the possibility of maintaining the formation can be determined from the maneuver planes and directions as described in Remark 3.3. Figure 9 shows a flowchart of the algorithm for obstacle avoidance and formation keeping. Initially, each UAV in the formation moves toward a goal point. When the obstacle is detected, the collision avoidance maneuvers are initiated by each UAV as described in Remarks 3.1 and 3.2. If necessary, the vehicles break formation as described in Remark 3.3, and the best avoidance path (direction and plane) is selected for each group. Note that collision avoidance maneuvers will not be employed if the collision avoidance has been completed according to Definition 3.3.

If the collision avoidance maneuvers for an obstacle have been completed, then the UAVs in the formation will continue with the mission or respond to the next obstacle. To prevent a false decision on the completion of collision avoidance, a time margin that determines the completion of collision avoidance is considered. The prevention of collisions between UAVs during the flight is considered in the following remark.

Remark 3.4 : (Prevention of Friendly Collisions). If two or more UAVs approach each other and are within the formation separation distance d_{FS}, then the UAVs share the same control command u for avoiding a collision among themselves after the completion of the original collision avoidance maneuvers; i.e.,

$$\text{For all UAV } j, \quad u_j = u_i \quad \text{if } \|r_i - r_j\| \le d_{FS} \qquad (44)$$

where UAV i is the vehicle in the formation that has completed the obstacle avoidance maneuvers first and r_i is the position vector of UAV i.

◇

Because all of the UAVs know the completion time of the avoidance maneuvers, collisions among the UAVs during formation recovery after the obstacle has been avoided may be successfully prevented using Eq. (44). The formation separation distance $d_{FS} (d_{FS} < d_C)$ should be selected through analysis, taking into account the dynamic constraints and the sensing capabilities of the UAVs.

IV. Numerical Simulations

A. Simulation Conditions

Numerical simulations were performed to test the performance of the proposed collision avoidance algorithm. Several assumptions were made for the simulations. First, it was assumed that the obstacles were stationary or moving with a constant ground speed and direction. In addition, it was assumed that all UAVs moved with a constant ground speed and their velocity vectors and positions coming through embedded GPS/INS system. If the on-board sensors of UAV can pick the information autonomously, then it is very effective in long-range military mission. In order to decide numerical setup, the circumstance used in UAV's air-traffic management problem is considered. The ground speeds of UAVs and the moving obstacles were set 56 m/s ($\approx$ 110 KIAS) [55]in this study. The U.S. Federal Aviation Administration (FAA) requires a minimum horizontal separation between aircraft of 5 nm (9,260 m) in en route airspace and 3 nm (5,550 m) in terminal airspace and a minimum vertical separation between aircraft of 1,000 feet (304 m) in en route airspace. [56] These standards were intended for large transportmanned aircraft. Therefore, these standards were scaled for the UAVs considered in this study. The safety radius d_C for the UAV was chosen to be 2,900 m based on the ratio of the ground speeds of the UAVs and those of conventional large transport manned aircraft, which are typically 900-1,000 km/h.

In Section IV-B, the formation-keeping strategy is validated with scenarios involving multiple obstacles. To show the performance of the strategy, the scenarios were in two dimensions (the XY-plane) so that the UAVs and the obstacles maneuvered using only heading angle commands, and the target point, the UAVs and the obstacles were all at the same altitude.
In Section IV-C, the influence of the time delay during collision avoidance is analyzed for the case of backward obstacle.
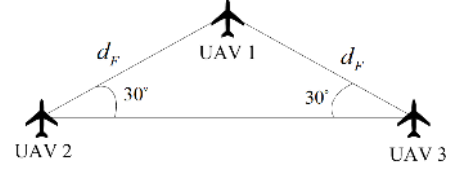

Fig. 10. Initial triangular formation with three UAVs.

In Section IV-D, the results for a formation splitting problem with a moving obstacle in two dimensions (the XY-plane) are presented.
The three UAVs were initially flying in a triangular formation, as shown in Fig. 10. Table I summarizes the parameters used in the simulations.

B. Collision Avoidance with Moving Obstacles

In this section, the results of numerical simulations are presented to demonstrate the proposed collision avoidance scheme for multiple UAVs in formation avoiding moving obstacles. The collision avoidance envelope with constraints is also analyzed.

The relative distances between the UAVs and the obstacles are shown in Fig. 11, and the angular rates of the UAVs are shown in Fig. 12. The momentary peaks in the yaw rates may be the result of the transitions in the guidance law between goal point tracking and collision avoidance. The relative distances exceeded the collision radius d_C at all times, and the angular rate constraints were satisfied. The obstacle approaching from ahead, obstacle 1, was avoided first, and then the obstacle approaching from right to left, obstacle 2, was successfully avoided, as indicated with the thick solid lines. Using the strategy in Remarks 3.1 and 3.2, collision avoidance was successfully completed using the XY-plane, as shown in Fig. 13. Figure 14 shows the values of S for UAVs 1-3 in the XY- and XZ-planes. At the time that each obstacle was detected, the values of S in both the XY- and XZ-planes were positive, and therefore the obstacles were avoidable. Figure 15 presents the sequence of movements of the three UAVs to avoid two obstacles moving with different velocity vectors in the XY-plane. When the obstacles overlapped, the outermost candidate vector was used as a desired relative velocity vector to avoid a collision.

The moving obstacle approaching from the head and tail of the UAV were avoided as shown in Fig.16 and Fig. 17, respectively.

Detection radius, d_{RG}	7,000 m
Collision radius, d_C	2,900 m
Velocity of UAV, v_u	56 m/s
Velocity of dynamic obstacle, v_o	56 m/s
Pitch rate limit, q_{lim}	15 deg/s
Yaw rate limit, r_{lim}	15 deg/s

TABLE I
PARAMETERS USED FOR SIMULATIONS

Initial position	Formation keeping : in Section IV-B	Formation splitting : in Section IV-D
UAV 1	(-13,000　　0)	(-8,000　-1,000)
UAV 2	(-13,450　779)	(-8,900　-1,559)
UAV 3	(-13,450　-779)	(-8,900　-1,559)
d_F (m)	900	1,800

TABLE II
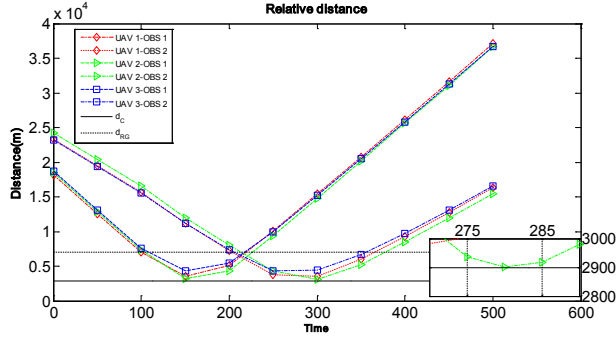INITIAL CONDITIONS OF THE UAVS FOR THE SIMULATIONS. (SECTIONS IV-B AND IV-D)

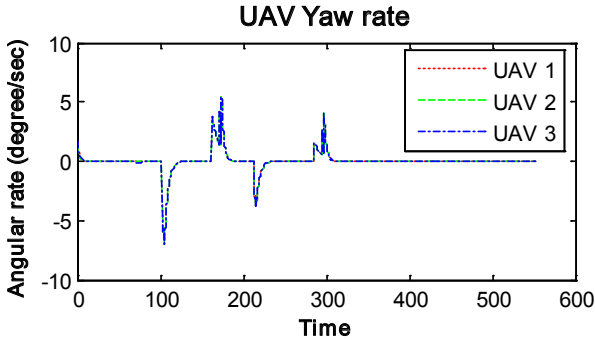Fig. 11. Relative distances between the UAVs and the two moving obstacles.

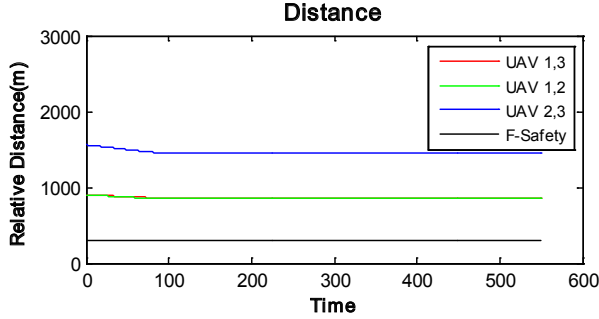Fig. 12. Angular rates of the UAVs. (two moving obstacles)

Fig. 13. Relative distances between UAVs 1,2 and 3. (two moving obstacles)

C. Influence of the Time Delay in Collision Avoidance

In this section, the influence of the time delay during collision avoidance is analyzed for the case of obstacle coming from the backside. Assuming that the UAVs are fully controlled and operated by ground control operators, then there exists an issue of delay incurred before the ground control operator receives visual information and takes appropriate action. Therefore, the collision avoidance envelope could change before the UAV gets to re-task its path. Considering the synchronization and time delays in communication and control, the previous simulation case of the obstacle coming from the backside is repeatedly performed with the time delay. Figure 18 shows the trajectories of the 3 UAVs for the case of the left-backward obstacle with (a) 1.5 seconds delay, (b) 3.0 seconds delay, respectively. Comparing the results of the
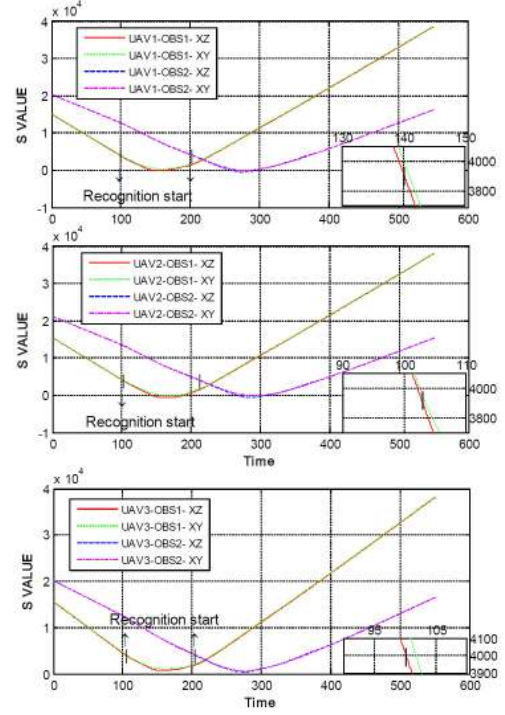

Fig. 14. Collision avoidance margin (S) values vs. time (two moving obstacles)
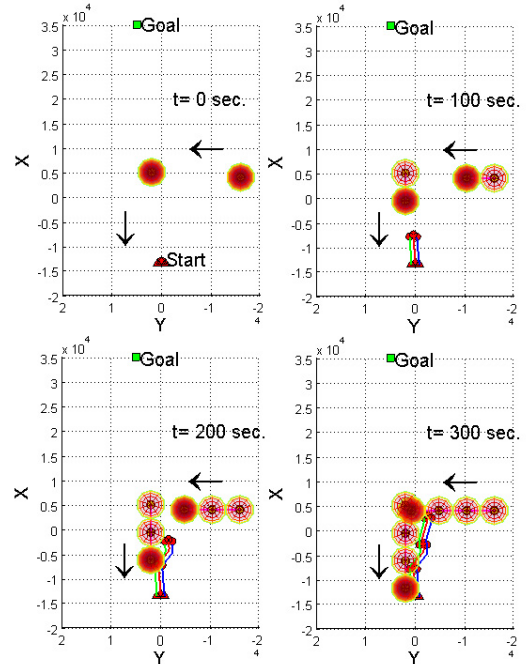

Fig. 15. Collision avoidance maneuvers of the UAVs with two moving obstacles. (in the XY-plane)
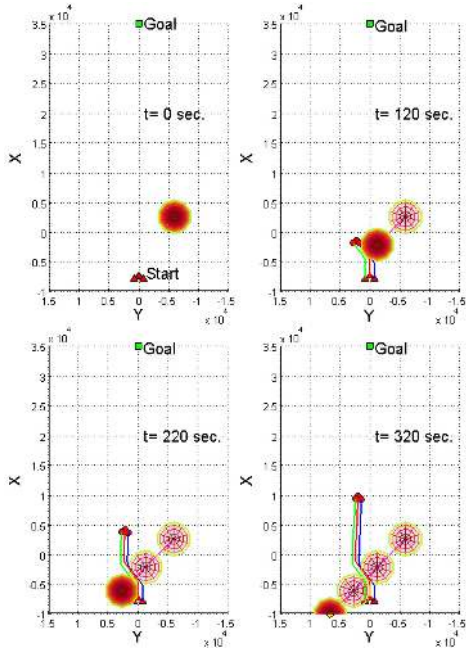
Fig. 16. Trajectories of the 3 UAVs for the case of the right-frontward obstacle.
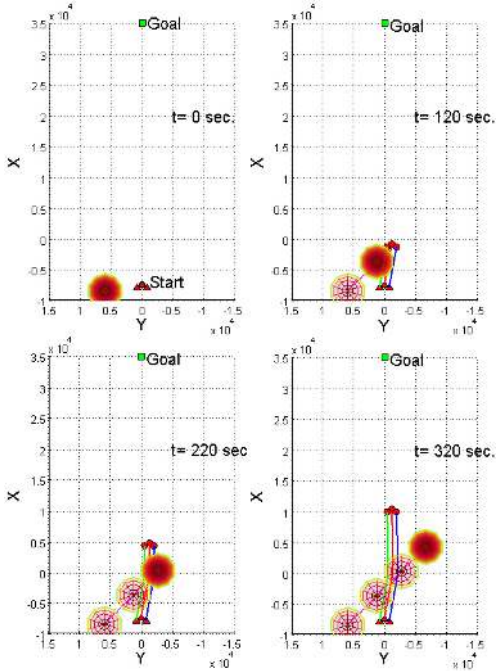

Fig. 17. Trajectories of the 3 UAVs for the case of the left-backward obstacle.
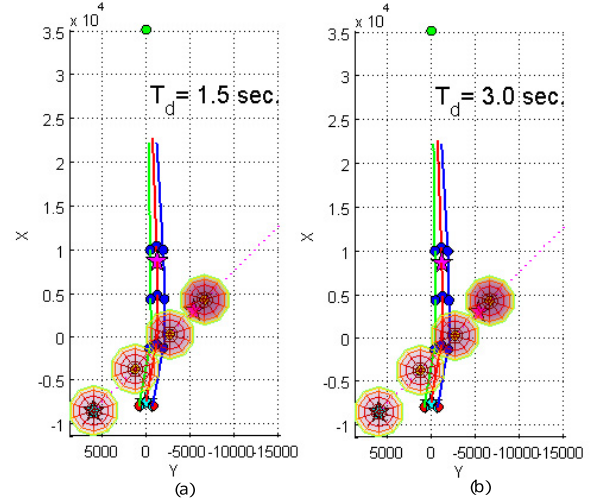

Fig. 18. Trajectories of the 3 UAVs for the case of the left-backward obstacle with (a) 1.5 seconds delay (b) 3.0 seconds delay.
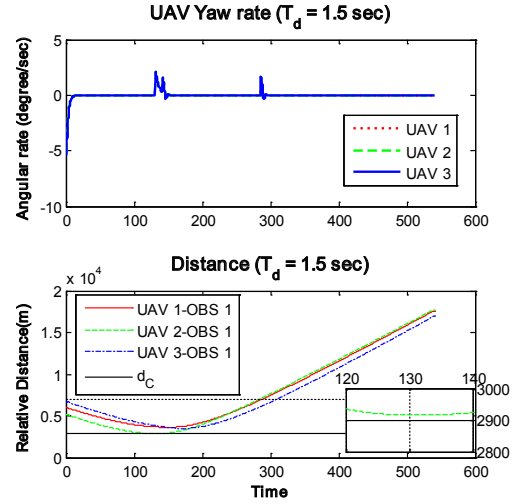

Fig. 19. Yaw rates of the 3 UAVs and relative distance for the case of the left-backward obstacle with 1.5 seconds delay.

trajectories of UAVs with various amount of time delay, any noticeable difference was not found. In order to check the influence of time delay, yaw rates of UAV and the relative distance between UAV and obstacle are shown in Fig.19 and Fig. 20, for each case. Due to the results of angular rate, fluctuation of yaw rate is occurred in 3.0 seconds time delay case. However, it is confirmed that the relative distance satisfies the collision radius criteria. Therefore, the proposed collision avoidance strategy is effective with conventional time delay under 3.0 seconds, [55]. Of course, it can be inferred that flying quality and collision avoidance performance will be deteriorated if time delay is getting longer.

D. Formation Splitting with a Moving Obstacle

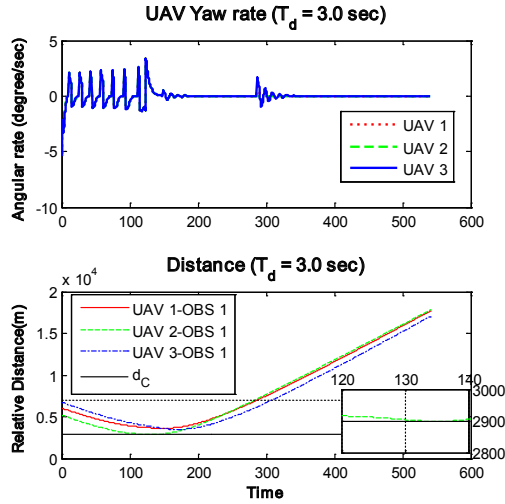In this section, simulation results for a different scenario are presented to show that a formation can be split using

Fig. 20. Yaw rates of the 3 UAVs and relative distance for the case of the left-backward obstacle with 3.0 seconds delay.
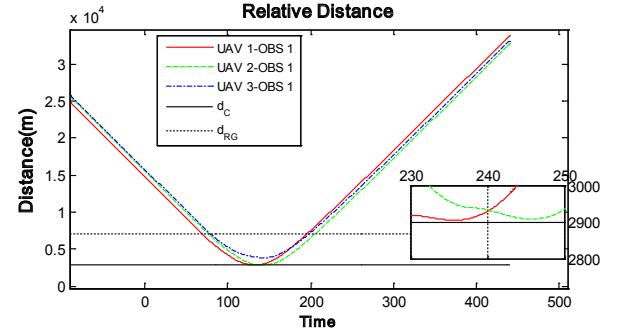

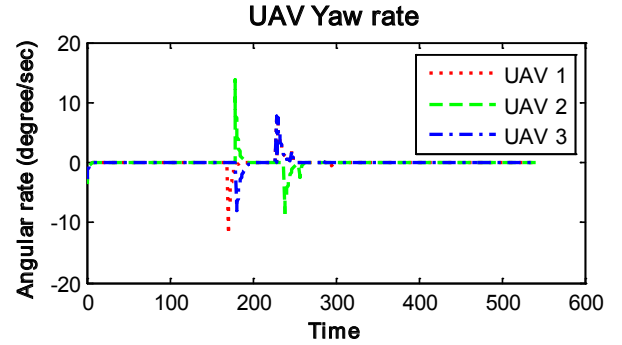Fig. 21. Relative distances between the UAVs and an obstacle with formation splitting.

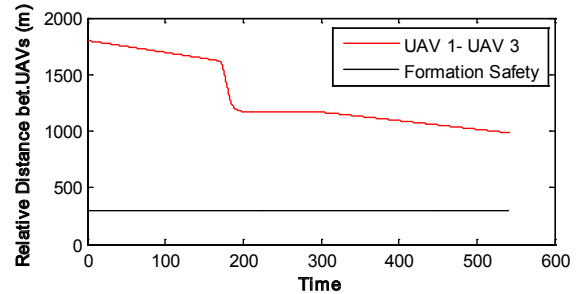Fig. 22. Angular rates of the UAVs with formation splitting.

Fig. 23. Relative distances between UAV 1 and UAV 3 with formation splitting.

the relative line-of-sight vectors between the UAVs and the obstacles. The collision avoidance envelope is also analyzed. The splitting strategy is evaluated using various sets of initial conditions and compared with the formation-keeping case. Table II summarizes the initial conditions of the UAVs. Note that the separation distance between the UAVs in formation was 1,800 m, and this distance doubled when the formation was split. The same constraints that were used in section IV-C were used here. The relative distances between the UAVs and the obstacles, shown in Fig. 21, and the yaw rates, shown in Fig. 22, confirm successful collision avoidance. Note that the relative distance between UAV 1 and UAV 3 was sufficient and the formation safety logic after obstacle avoidance was not activated, as shown in Fig. 23. Figure 24 shows the values of S during the maneuvers. The values in both the XY- and XZ-planes were positive for each UAV at the time the obstacle was detected. Therefore, the obstacle was avoidable, and collision avoidance was successfully completed using XY-plane maneuvers according to the strategy in Remark 3.1. The splitting of the formation in to the 2-vehicle formation and the single vehicle using the strategies in Remarks 3.2 and 3.3 performed well. Figure 25 shows the sequence of movements of the UAVs. One of the UAVs broke from the formation using the formation splitting scheme described in Remark 3.2. The opposite side of the tangent line was chosen as the desired vector for UAV 2. However, using Eq. (39) in Remark 3.3 for formation keeping, in which the UAVs choose the same maneuver direction, the formation consisting of UAV 1 and UAV 2 was maintained during the collision-avoidance maneuvers.

V. CONCLUSIONS AND FUTURE RESEARCH

A strategy was developed for multiple UAVs in formation to avoid collisions with obstacles. Lyapunov theory was used to analyze the stability of the proposed guidance law for collision avoidance. Dynamic constraints on the motion of the UAVs

and the detection capabilities of the UAVs were considered in the analysis of the envelope for collision avoidance. The envelope for collision avoidance guaranteed successful collision avoidance because the dynamic constraints were included. Formation keeping and splitting strategies were developed using the collision avoidance envelope. Numerical simulations were performed to demonstrate the performance of the collision avoidance algorithm and formation keeping/splitting strategy. The proposed collision avoidance strategy is a sense-and-avoid approach, which is more practical for UAVs in avoiding collisions with moving obstacles. The collision avoidance strategy applies not only to a single UAV but also to multiple UAVs. Therefore, this strategy can be effective for actual operation of UAVs. Extending the envelope analysis to consider changes in velocity for the UAVs is a topic for further study.
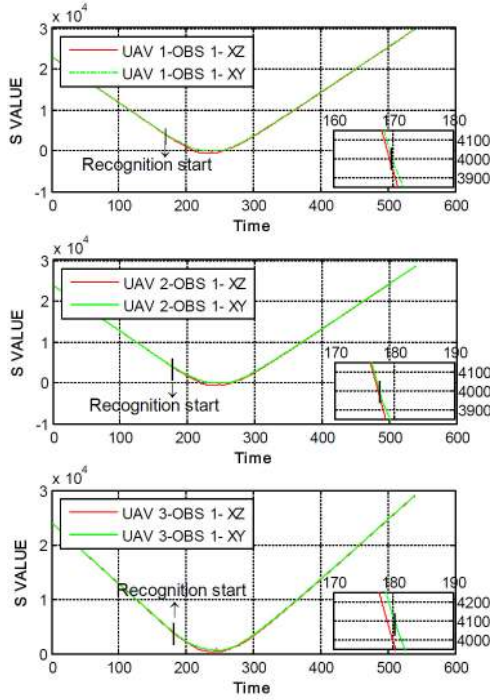
Fig. 24. Collision avoidance margin (S) values vs. time with formation splitting.
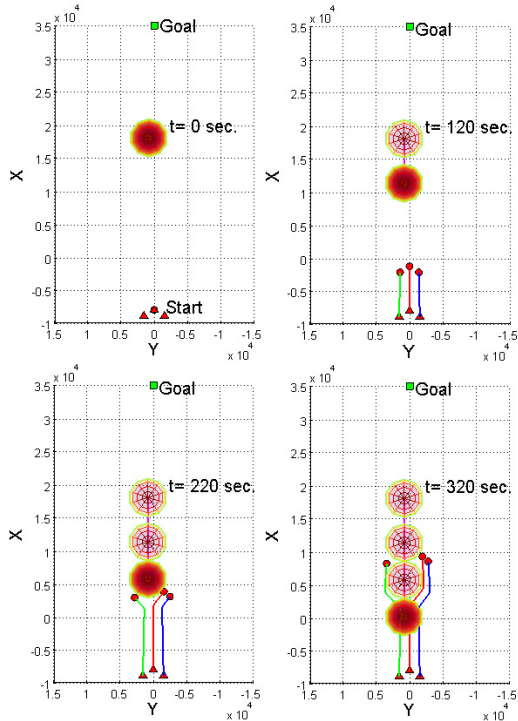

Fig. 25. Trajectories of the 3 UAVs with formation splitting.

REFERENCES

[1] R., M., Murray, "Recent Research in Cooperative Control of Multivehicle System," *Journal of Dynamic Systems, Measurement, and Control*, Vol. 129, No. 9, pp. 571-583, 2007.

[2] J., G., Manathara, and D. Ghose "Rendezbous of Multiple UAVs with Collision Avoidance Using Consensus," *Journal of Aerospace Engineering*, Vol. 25, No. 4, pp. 480-489, 2012.

[3] G., B., Ladd, and G., L., Bland "Non Military Applications for Small UAS Platforms," *AIAA Infotech@Aerospace*, Seattle, WA, April, 2009.

[4] R., M., Murray, K., J., Astrom, S., P., Boyd, R., W., Brockett, and G., Stein "Future Directions in Control in an Information-Rich World," *IEEE Control Systems Magazine*, No. 4, pp. 20-33, 2003.

[5] P., R., Chandler, M., Patcher, and S., Rasmussen "UAV Cooperative Control," *Proceedings of the American Control Conference*, Arlington, VA, June, 2001.

[6] L., E., Parker "Designing Control Laws for Cooperative Agent Teams," *Proceedings of IEEE International Conference on Robotics and Automation*, Atlanta, GA, May, 1993.

[7] E., Lavretsky, "F/A-18 Autonomous Formation Flight Control System Design," *AIAA Guidance, Navigation, and Control Conference*, Monterey, CA, Aug., 2002.

[8] J., Choi, and Y., Kim, "Fuel Efficient Formation Flight Control Design Based on Energy Maneuverability," *AIAA Guidance, Control and Dynamics*, Vol. 31, No. 4, pp. 1145-1150, 2008.

[9] Y., F., Zou, P., R., Pagilla, and R., T., Ratliff, "Distributed formation flight control using constraint forces," *Journal of Guidance, Control and Dynamics*, Vol. 32, No. 1, pp. 112-120, 2009.

[10] D., E., Kirk, "Optimal Control Theory : An Introduction," *Prentice-Hall Inc*, Englewood Cliffs, NJ, 1970.

[11] F., L., Lewis, "Applied Optimal Control and Estimation," *Prentice-Hall Inc*, Englewood Cliffs, NJ, 1992.

[12] E., Boivin, A., Desbiens, and E., Gagnon, "UAV Collision Avoidance using Cooperative Predictive Control," *16th Mediterranean Conference on Control and Automation*, Ajaccio, France. June, 2008.

[13] Y., Kuwata, and J. How, "Three Dimensional Receding Horizon Control for UAVs," *AIAA Guidance, Navigation, and Control Conference*, Providence, RI, Aug, 2004.

[14] W. B. Dunbar, and R., M., Murray, "Distributed receding horizon control for multi-vehicle formation stabilization," *Automatica*, No. 42, pp. 549-558, 2005.

[15] T., Kevickzy, F., Borrelli, K., Fregene, D., Godbole and G. J., Balas, "Decentralized receding horizon control and coordination of autonomous vehicle formations," *IEEE Transaction on Control System and Technology*, Vol. 16, No. 1, pp. 19-33, 2008.

[16] W., Kwon, and S. Han, "Receding horizon control : Model Predictive control for state models," '*Springers*, London, 2005.

[17] N., Smith, R. G. Cobb., and S. J. Pierce, "Optimal Collision Avoidance Trajectories for Unmanned/Remotely Piloted Aircraft," *AIAA Guidance, Navigation, and Control*, Boston, MA, Aug., 2013.

[18] N., Smith, R. G. Cobb., and S. J. Pierce, "Optimal Collision Avoidance Trajectories via Direct Orthogonal Collocation for Unmanned/Remotely Piloted Aircraft Sense and Avoid Operations," *AIAA Guidance, Navigation, and Control*, National harbor, MD, Jan., 2014.

[19] P., B., Sujit, and R., Beard, "Multiple UAV Path Planning using Anytime Algorithms," *American Control Conference*, St. Louis, MO, June, 2009.

[20] J., M., George, P.,B Sujit J., B., Sousa, and F., L., Pereira, "Coalition Formation With Communication Ranges and Moving target," *American Control Conference*, St. Louis, MO, June, 2009.

[21] J., G., Manathara, P., B., Sujit, and R., Beard, "Multiple UAV Coalitions for a Search and Prosecute Mission," *Journal of Intelligent Robot System*, No. 62, pp.125-158, 2011.

[22] O., M., Shehory, "Methods for task allocation via agent coalition formation," *Artificial Intelligence*, Vol. 101, No. 12, pp. 165-200, 1998.

[23] H., B., Duan and S., Q., Liu, "Non-linear dual-mode receding horizon control for multiple unmanned air vehicles formation flight based on chaotic particle swarm optimization," *IET Control Theory and Application*, Vol. 4, No. 11, pp. 2565-2578, 2010.

[24] H., B., Duan, S., Q., Liu, and G., Ma, "Hybrid Particle Swarm Optimization and Genetic Algorithm for Multi-UAV Formation Reconfiguration," *IEEE Computational Intelligence Magazine*, No. 8, pp. 16-27, 2013.

[25] J., Chen, W., Zha, Z., Peng, and J., Zhang, "Cooperative Area Reconnaissance for Multi-UAV in Dynamic Environment," *9th Asian Control Conference (ASCC)*, Istanbul, June, 2013.

[26] J., Barraquand, B., Langlois, and J.C., Latombe, "Numerical Potential Field Techniques for Robot Path Planning," *IEEE Transactions on Systems, Man, and Cybernetics*, Vol. 22, No.2, pp. 224-241, 1992.

[27] Y., Lee, and Y., Kim, "Distributed Unmanned Aircraft Collision Avoidance using Limit Cycle," *ICCAS International Conference on Control Automation and Systems*, Gyeonggido, Korea, Oct., 2011.

[28] E., P., Lopes, E., P., Aude, J., T., Silveira, and H., Serdeira, "Obstacle Avoidance Strategy Based on Adaptive Potential Fields Generated by an Electronic Stick," *Intelligent Robots and Systems*, Edmonton, Canada, Aug., 2005.

[29] A., Oguz, E., Duymaz, 'Artificial Potantial Field Based Autonomus UAV Flight in Dynamic Environment," *16th AIAA Aviation Technology, Integration, and Operations Conference*, Washington, D.C., June, 2016.

[30] Y., Koren and J., Borenstein, "Potential field methods and their inherent limitations for mobile robot navigation," *Proceedings of the IEEE International Conference on Robotics and Automation*, Sacramento, CA, April, 1991.

[31] T., Paul, T., Krogstad, and J., Gravdahl, "UAV formation flight using 3D potential field," *16th Mediterranean Conference on Control and Automation*, Ajaccio, France, June, 2008.

[32] Y., Chen, J., Yu , X., Su, and G., Luo, "Path Planning for Multi-UAV Formation," *Journal of Intelligent and Robotic Systems*, Vol. 77, No. 1, pp. 229-246, 2015.

[33] X., Prats, L., Delgado, J., Ramirez, P., Royo, and E., Pasto, "Requirements, issues, and challenges for sense and avoid in Unmanned Aircraft Systems," *Journal of Aircraft*, Vol. 49, No. 3, pp. 677-687, 2012.

[34] A., Chakravarthy, and D., Ghose, "Obstacle avoidance in a dynamic environment- A collision cone approach," *IEEE Transactions on Systems, Man, and Cybernetics*, Vol. 28, No. 5, pp. 562-574, 1998.

[35] J., Goss, R., Rajvanshi, and K., Subbarao, "Aircraft conflict detection and resolution using mixed geometricand collision cone approaches," *AIAA Guidance, Navigation, and Control Conference*, Providence, RI, Aug., 2004.

[36] Y., Watanabe, A. J., Calise, and E., Johnson, "Vision-based obstacle avoidance for UAVs," *AIAA Guidance, Navigation, and Control Conference*, Hilton Head, SC, Aug., 2007.

[37] H., Choi, Y., Kim, and I., Hwang, "Vision-based Reactive Collision Avoidance Algorithm for Unmanned Aerial Vehicle," *AIAA Guidance, Navigation, and Control Conference*, Portalnd, OR. Aug., 2011.

[38] E., Portilla, A., Fung, W., Chen, and O., Shakernia, "Sense And Avoid (SAA) and Traffic Alert and Collision Avoidance System (TCAS) Integration for Unmanned Aerial Systems(UAS)," *AIAA Infotech@Aerospace Conference*, Rohnert Park, CA, May, 2007.

[39] G., Fasano, D., Accardo, and A., Moccia, "Multi-sensor-based fully autonomous non-cooperative collision avoidance system for unmanned air vehicles," *Journal of Aerospace Computing, Information,and Communication*, 5, pp. 338-360, 2008.

[40] H., S., Shin, A., Tsourdos, B. A., White, M., Shanmugavel, and M. J., Tahk, "UAV conflict detection and resolution for static and dynamic obstacles," *AIAA Guidance, Navigation, and Control Conference*, Honolulu, HI, Aug., 2008.

[41] B., A., White, H., S., Shin, and A., Tsourdos, "UAV Obstacle Avoidance using Differential Geometry Concepts," *IFAC World Congress*, Milano, Italy, Aug., 2011.

[42] A., Mujumdar and R., Padhi, "Reactive Collision Avoidance using Nonlinear Geometric and Differential Geometric guidance," *Journal of Guidance, Control, and Dynamics*, Vol. 34, No. 1, pp. 303-310, 2011.

[43] E., Lalish, E., and A., Morgansen, "Distributed reactive collision avoidance," *Auton Robot*, 32, pp. 207-226, 2012.

[44] J., S., Bellingham, M., Tillerson, M., Alighanbari, and J., P., How, "Cooperative Path Planning for Multiple UAVs in Dynamic and Uncertain Environments," *Proceedings of the 41st IEEE Conference on Decision and Control* , Las Vegas, NV, Dec., 2002.

[45] S., Han, H., Bang, C., Yoo, "Proportional navigation-based collision avoidance for uavs," *International. Journal of Control, Automation, and Systems*, Vol. 7, No. 4, pp.553-565, 2009.

[46] K., P., Bollino, and L. R., Lewis, "Collision-free Multi-UAV Optimal Path Planning and Cooperative Control for Tactical Applications," *AIAA Guidance, Navigation and Control Conference*, Honolulu, HI., Aug., 2008.

[47] J., Seo, Y., Kim, S., Kim, and A., Tsourdos, "Consensus-based Reconfigurable Controller Design for UAV Formation Flight," *Journal of Aerospace Engineering, Proceedings of the Institution of Mechanical Engineers Part G*, Vol. 226, No. 7, pp.817-829, 2012.

[48] A., Yang, W., Naeem, and M., Fei "Decentralised Formation Control and Stability Analysis for Multi-vehicle Cooperative Manoeuvre," *IEEE/CAA Journal of Automatica SINICA*, Vol. 1, No. 1, pp. 92-100, 2014.

[49] E., Garcia, and D., W., Casbeer "Cooperative Task Allocation for Unmanned Vehicles with Communication Delays and Conflict Resolution,"

Journal of Aerospace Information Systems, Vol. 13, No. 2, pp. 67-79, 2016.

[50] M., K., Kuchar and, L., C., Yang, "A Review of Conflict Detection and Resolution Modeling Methods," *IEEE Transactions on intelligent Transportation Systems*, Vol. 1, No. 4, pp. 179-189, 2000.

[51] A., Desilles, and H., Zidani, "Collision analysis for an UAV," *AIAA Guidance, Navigation and Control Conference*, Minneapolis, MN., Aug., 2012.

[52] J., Farinella, C., Lay, and S., Bhandari, "UAV Collision Avoidance using a Predictive Rapidly-Exploring Random Tree(RRT)," *AIAA Infotech@Aerospace Conference*, San Diego, CA, Jan., 2016.

[53] D., Luo, T., Zhou, and S., Wu, "Obstacle avoidance and formation regrouping strategy and control for UAV formation flight," *10th IEEE International Conference on Control and Automation*, Hangzhou, China, June, 2013.

[54] J., K., Cooper, N., D., Richards, J., D., Schierman, and D., Neal, "A Sense and Avoid System Unmanned Aircraft in Formation Flight," *AIAA Guidance, Navigation and Control Conference*, National Harbor, MD., Jan., 2014.

[55] D. R., Schmitt, S., Kaltenhauser, and B., Keck, "Real time Simulation of Integration of UAV's into Airspace," *26th Congress of the International Council of the Aeronautical Sciences*, Anchorage, AL, Sep., 2008.

[56] Federal Aviation Administration., "Introduction to TCAS II. Version 7.1," *U.S. Department of Transportation*, Feb., 2011.